

## ORIGINAL RESEARCH

# Expressions of miR-96-5p, miR-29b-3p, and Their Target Gene THBS1 in Clear Cell Renal Cell Carcinoma and Sunitinib Resistance

Shenghua Wu, MM; Ying Wang, MM

### ABSTRACT

**Objective** • Clear cell renal cell carcinoma (ccRCC) is the most prevalent subtype of RCC and comprises approximately 70% of all RCC cases, with high incidence and metastatic relapse. Sunitinib is a first-line drug for treating patients with metastatic RCC but drug resistance inevitably occurs in a vast majority of patients after 15 months of systematic treatment. Herein, we attempted to explain the possible mechanism of sunitinib resistance in ccRCC.

**Methods** • Two expression profiles with accession numbers GSE64052 and GSE76068 in the GEO were utilized to identify differentially expressed genes ( $|\log_2FC| \geq 1$  with adjusted  $P < .05$ ) between sunitinib sensitivity and sunitinib resistance in ccRCC. The study included tumor and matched non-tumor kidney tissues obtained from 64 ccRCC patients who underwent nephrectomy before adjuvant therapy.

**Results** • The gene expression profiles of GSE64052 and GSE76068 datasets yielded 92 and 66 differentially expressed genes between sunitinib sensitivity and sunitinib resistance in ccRCC, respectively. The PPI analysis revealed *CTGF*, *RSAD2*, and *THBS1* as hub genes among which only *THBS1* was found to be correlated with the

survival of ccRCC patients. *miR-96-5p* and *miR-29b-3p* were common miRNAs targeting *THBS1* and correlated with the survival of ccRCC patients. The luciferase activity assays demonstrated *THBS1* as the target gene of *miR-96-5p* and *miR-29b-3p*. Results of qRT-PCR provided evidence of higher expressions of *miR-96-5p* and *miR-29b-3p* with a lower expression of *THBS1* in tumor kidney tissues than matched non-tumor kidney tissues and in tumor kidney tissues of responders than those of non-responders. More specifically, elevated expressions of *miR-96-5p*, *miR-29b-3p*, and a declined expression of *THBS1* were observed in tumor samples with advanced ccRCCs and higher Fuhrman grades. Pearson correlation analysis yielded significantly negative correlations between *miR-96-5p* and *THBS1* ( $P < .006$ ,  $r = -0.339$ ), between *miR-29b-3p* and *THBS1* ( $P < .05$ ,  $r = -0.421$ ).

**Conclusion** • Our study suggests that *miR-96-5p*- and *miR-29b-3p*-mediated *THBS1* inhibition is associated with sunitinib resistance in ccRCC, offering a better understanding of the mechanism elucidating acquired drug resistance in ccRCC. (*Altern Ther Health Med*. 2024;30(7):268-273).

Shenghua Wu, MM; Ying Wang, MM, Department of Urology Surgery, Zhoushan Branch Shanghai Ruijin Hospital, Zhoushan, Zhejiang, China.

Corresponding author: Ying Wang, MM  
E-mail: [wangying060818@126.com](mailto:wangying060818@126.com)

### INTRODUCTION

Renal cell carcinoma (RCC) is a cancer caused by renal epithelial cells and has become one of the most common urogenital tumors. In the cancer case report, globally, 5% of men and 3% of women are newly diagnosed with RCC,<sup>1</sup> and the adults over 60-70 years are more likely to suffer from RCC.<sup>2</sup> According to WHO classification, RCC mainly includes three subtypes defined histologically, including clear

cell renal cell carcinoma (ccRCC), papillary RCC, and chromophobe RCC.<sup>3</sup> In 2018, the incidence of papillary RCC and chromophobe RCC was 7% - 14% and 6% - 11%, respectively.<sup>4</sup> As the most common subtype of RCC, ccRCC is an aggressive cancer originating from the proximal tubular epithelium and is responsible for approximately 80% of adult cases in the clinic. Cancer metastasis often occurs in ccRCC and 25% - 30% of patients are already metastasized when they are first diagnosed with ccRCC. The ccRCC is associated with high mortality due to its metastatic form and relapsed ccRCC following surgery, leading to about 90,000 deaths annually worldwide.<sup>5-7</sup> Furthermore, the patients with advanced RCC present poor prognosis, with a 5-year survival only among 11.7% of the patients.<sup>8</sup>

Currently, sunitinib and pazopanib are the main first-line treatments in metastatic RCC and axitinib and sorafenib

are considered second-line agents that contribute to an increase in the chances of progression-free survival.<sup>9, 10</sup> As an inhibitor of vascular endothelial growth factor pathway, sunitinib has been proven to prolong the median disease-free survival of patients with RCC at high risk of tumor recurrence after nephrectomy,<sup>11</sup> and sunitinib therapy before cytoreductive nephrectomy improved overall survival of metastatic RCC. However, drug resistance often occurs within 6-15 months of treatment, resulting in unsatisfactory overall survival.<sup>12, 13</sup> Hence, it is necessary to explore the underlying mechanism of sunitinib resistance in the treatment of ccRCC.

MicroRNAs (miRNAs) are small non-coding RNAs that play a vital role in the post transcriptional regulation of gene expression and participate in the development of various diseases by regulating cell growth, differentiation, development, and apoptosis.<sup>14</sup> Previous studies involving transcriptomic analyses of miRNAs based on their presence in the blood or urine revealed divergent mechanisms of drug resistance related to targeted therapeutic options like sunitinib in ccRCC.<sup>15, 16</sup> Large numbers of differentially expressed miRNAs in metastatic RCC presenting marked sensitivity or resistance to sunitinib have been identified, such as *miR-4731-5p* and *miR-362-3p*.<sup>17, 18</sup>

In this paper, we performed an analysis of miRNA-mRNA profile related intrinsic sunitinib resistance in ccRCC that may not only help to monitor and follow sunitinib treatment but also allow us to identify ccRCC patient groups who are most likely to benefit from treatment other than sunitinib.

## MATERIALS AND METHODS

### Data sources and processing

Two expression profiles were obtained from the Gene Expression Omnibus (GEO, <http://www.ncbi.nlm.nih.gov/geo>) database with accession number as GSE64052 and GSE76068, respectively. The GSE64052 dataset that was processed on the GPL570 platform (public on May 21, 2015) encompasses 4 ccRCC samples of patient-derived mouse xenografts resistant to sunitinib (ranging from GSM1563514 to GSM1563517) and 5 ccRCC samples of sensitive sunitinib (ranging from GSM15636509 to GSM1563513). The GSE76068 dataset that was processed on the GPL6885 and GPL10558 platform (public on Dec 17, 2015) contained 8 ccRCC samples of patient-derived mouse xenografts resistant to sunitinib (ranging from GSM1973629 to GSM1973636) and 8 ccRCC samples of sensitive sunitinib (ranging from GSM1973621 to GSM1973628). The genes deemed differentially expressed between sunitinib sensitivity and sunitinib resistance in ccRCC should fulfill log2-fold change  $|\log_2FC| \geq 1$  and the adjusted  $P < .05$  by using the limma Bioconductor R package.

### Protein-protein interaction (PPI) analysis

The PPI of genes differentially expressed between sunitinib sensitivity and sunitinib resistance in ccRCC was

analyzed using the STRING (<https://string-db.org/>). The results of the PPI network analysis were presented using Cytoscape software (v3.9.0), where a minimum effective binding score was 0.4, otherwise the sparse genes were removed. The cytoHubba plugin in the Cytoscape was applied to calculate the degree values of nodes in the PPI network, and a higher degree value indicates a more significant role played in the network's topology. When nodes have a degree value  $\geq 10$ , the corresponding genes are denoted as hub genes.

### miRNA-hub gene interactions

Venn intersection analysis was performed to sort out common genes among differentially expressed genes between sunitinib sensitivity and sunitinib resistance in the GSE64052 and GSE76068, and hub genes. The hub genes obtained above were imported into the StarBase (<https://starbase.sysu.edu.cn/index.php>) and TargetScan (<http://www.targetscan.org/>) databases to predict miRNA-mRNA interactions. Common miRNAs targeted by hub genes were Venn-intersected.

### Survival and co-expression analysis

The hub genes and their candidate miRNAs were imported into the Pan-cancer function of the StarBase database (<https://starbase.sysu.edu.cn/panCancer.php>) in which the correlation between the expressions of hub genes, their candidate miRNAs, and survival, as well as their co-expressions were assessed.

### Luciferase activity assays

The pMIR-Report luciferase reporter cassettes (RiboBio, Guangzhou, China) spanning the human THBS1 3'UTR containing either wild-type or the mutated binding sites of *miR-96-5p* or *miR-29b-3p* were delivered into HEK293T cells (ATCC, USA) in the presence of *miR-96-5p* or *miR-29b-3p* mimic. The luciferase activity was detected using the Dual-Luciferase assay kit (Promega) and analyzed using a GloMax20/20 Luminometer (Promega).

### Human tissue sample collection

The study included tumor and matched non-tumor kidney tissues obtained from 64 ccRCC patients who underwent nephrectomy at our hospital in 2017-2022. The inclusion criteria were ccRCC diagnosed according to World Health Organization classification of RCC,<sup>19</sup> and an age of 18 years or above. The exclusion criteria were previous adjuvant therapy or systemic treatments, presence of active autoimmune disease, use of immunomodulatory drugs, New York Heart Association class IV, or congestive heart failure within 1 year before screening. These patients enrolled in this study had a mean age of 63.46 years with range from 80 to 37 years, including 40 males and 24 females. The anatomic extent of the tumors was classified based on the tumor-necrosis-metastasis (TNM) staging system (stage I indicating T1-2N0M0; stage II indicating T2N0M0; stage III indicating T1-2N1M0 or T3N0-1M0;

stage IV indicating T4N0-2M0 or T1-4N2M0 or T1-4N0-2M1) and histological nuclear staging based on the Fuhrman grading system.<sup>20</sup> There were 39 patients with tumor size ≤ 4 cm and 25 with tumor size > 4 cm; 40 patients as stage I + II and 24 as stage III + IV; 4 as Fuhrman grade I, 28 as Fuhrman grade II, 20 as Fuhrman grade III, and 12 as Fuhrman grade IV; 63 without distant metastasis and 1 with distant metastasis. Among 64 patients, 19 cases had received post-operative treatment, at least two cycles of sunitinib monotherapy in the first line. Each cycle lasted for 6 weeks consisting of 4-week oral administration (50 mg sunitinib once daily) followed by 2-week off treatment. To manage the toxic effects, the dose of sunitinib could be reduced to 37.5 mg and then 25 mg during the first 4 weeks in each cycle. Their therapy outcome was assessed three months after the therapy initiation<sup>21</sup> by computed tomography, magnetic resonance imaging, or clinical progression or death, with the aid of the Response Evaluation Criteria for Solid Tumors (RECIST) criteria (version 1.1).<sup>22</sup> Among 19 patients, 11 patients reached partial or complete remission, grouped as the responder, while 8 patients were confirmed as stable diseases or progressive diseases, grouped as the non-responder. The study was approved by the Ethics Committee of Zhoushan Branch Shanghai Ruijin Hospital, and all patients provided a written consent prior to surgery.

RNA extraction and quantitative real-time PCR (qRT-PCR)

The kidney tissues were homogenated and then extracted with acetonitrile. Total RNA was extracted from kidney tissues using the TRIzol reagent (Invitrogen, USA) according to the manufacturer’s instructions. The first-strand cDNA was synthesized from 1 to 2 μg of total RNA using the PrimeScript RT Reagent kit (Takara, Dalian, China), respectively. The expression quantification of candidate hub genes was achieved by using the SYBR® Premix Ex Taq™ II (Tli RNaseH Plus) kit (Takara) with the aid of the quantitative thermal cycler 7500 Real-Time PCR-System (Applied Biosystem, USA). The cycle threshold (Ct) values of miRNA and mRNA expression were normalized to those of U6 and GAPDH, and results were then converted into fold change using the 2<sup>-ΔΔCt</sup> formula.

Statistical analysis

The statistical tests applied in this study included independent t test and Pearson correlation coefficients, with *P* < .05 denoting a significant difference. The GraphPad Prism 8.0 software (GraphPad Software, USA) was used for statistical tests and figure creation.

RESULTS

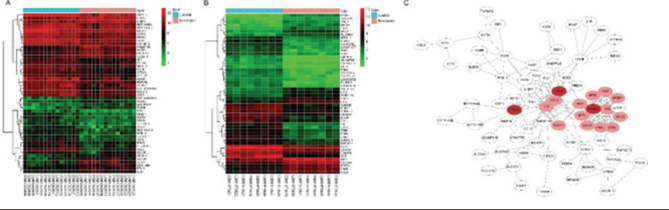
Identification of differentially expressed genes associated with ccRCC resistance to sunitinib

The gene expression profiles of GSE64052 and GSE76068 datasets were differentially analyzed, and those with |log2FC| ≥ 1 (adjusted *P* < .05) were deemed as differentially expressed genes between sunitinib sensitivity and sunitinib

Table 1. The Primer Sequences Used in the Real-Time PCR

Primer	Sequence (5'-3')	Length	Temperature
miR-96-5p	Forward: GCCGAGTTTGGCACTAGCAC	21	60.18
	Reverse: CTCAACTGGTGTCTGTGGA	18	60.03
miR-29b-3p	Forward: GCGGCGGTAGCACCATTGAAATC	24	60.61
	Reverse: GTCGTATCCAGTGCAGGGT	19	59.89
U6	Forward: AGGGGCCATCCACAGTCTTC	20	59.96
	Reverse: AACGCTTCACGAATTTGCGT	20	59.46
THBS1	Forward: AGAATGCTGTCTCGCTGTT	20	59.90
	Reverse: TTTCTTGCAAGGCTTTGGTCT	20	60.18
GAPDH	Forward: GTGTTCTACCCCAATGTG	20	60.11
	Reverse: CATCGAAGGTGGAAGAGTGG	20	59.59

Figure 1. Identification of differentially expressed genes associated with ccRCC resistance to sunitinib. Heatmaps showing expression diversity of representative 50 genes among differentially expressed genes between sunitinib sensitivity and sunitinib resistance in ccRCC after analyzing the gene expression profile of GSE64052 (A) and GSE76068 (B). Green color represents downregulation in response to sunitinib resistance and red color represents upregulation in response to sunitinib resistance. (C) Construction of PPI network. The PPI network encompasses 80 nodes with 195 edges, among which *IL6*, *CCL2*, *MX1*, *ISG15*, *IFIT2*, *IFIT3*, *OASL*, *RSAD2*, *CTGF*, *IFI27*, *IFI44L*, *THBS1*, *IFITM1*, *ISG20*, *MX2* (indicated as red nodes) owned degree values not less than 10 were deemed as core genes differentially expressed between sunitinib sensitivity and sunitinib resistance in ccRCC. Three more red nodes were regarded as hub genes.



resistance in ccRCC. Results showed 92 and 66 differentially expressed genes in ccRCC samples of patient-derived mouse xenografts between sunitinib sensitivity and sunitinib resistance, respectively. Among 92 differentially expressed genes, there were 60 genes downregulated and 32 genes upregulated in ccRCC resistance to sunitinib compared with ccRCC sensitivity to sunitinib (Figure 1A). Among 66 differentially expressed genes, there were 41 genes downregulated and 25 genes upregulated in ccRCC resistance to sunitinib compared with ccRCC sensitivity to sunitinib (Figure 1B).

Identification of hub genes associated with ccRCC resistance to sunitinib

After removal of 5 overlapping differentially expressed genes, 153 genes were obtained in total and subject to the PPI analysis in the STRING database. The PPI network is presented in Figure 1C, in which 80 nodes with 195 edges are obtained. *IL6*, *CCL2*, *MX1*, *ISG15*, *IFIT2*, *IFIT3*, *OASL*, *RSAD2*, *CTGF*, *IFI27*, *IFI44L*, *THBS1*, *IFITM1*, *ISG20*, and *MX2* owned degree values not less than 10 were deemed as core genes differentially expressed between sunitinib sensitivity and sunitinib resistance in ccRCC. Among these 15 core genes, *CTGF*, *RSAD2*, and *THBS1* as common



**Figure 2.** Common putative miRNAs targeting (A) *CTGF*, (B) *RSAD2*, and (C) *THBS1* in the StarBase and TargetScan databases. (D) The survival analysis of ccRCC patients (n = 517) based on the expressions of *miR-96-5p*, *miR-29b-3p*, and *THBS1*.

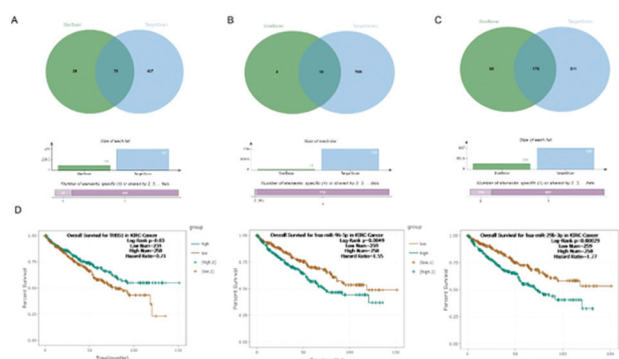
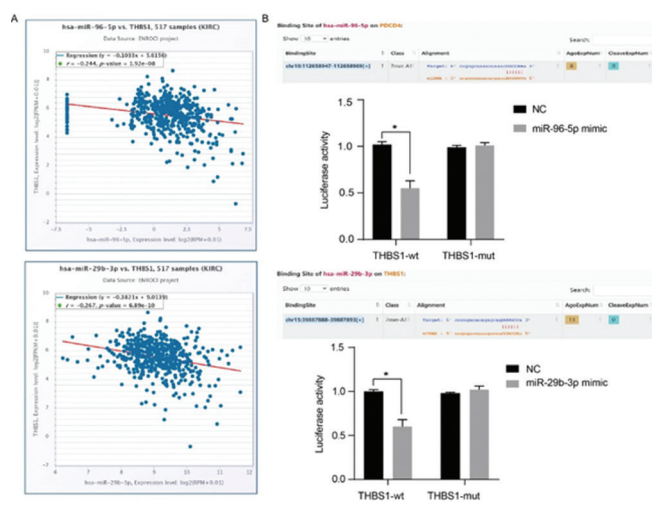


**Figure 3.** *THBS1* as the target gene of *miR-96-5p* and *miR-29b-3p*. (A) The miRNA-Target co-expression of *miR-96-5p*, *miR-29b-3p*, and *THBS1* in ccRCC patients (n = 517). (B) The putative binding sites of *miR-96-5p* and *miR-29b-3p* in the *THBS1* mRNA 3'UTR in the StarBase and luciferase activity detection of a luciferase reporter cassette spanning the human *THBS1* 3'UTR containing either wild-type or the mutated *miR-96-5p* or *miR-29b-3p* binding site in HEK293T co-transfected with *miR-96-5p* or *miR-29b-3p* mimic.



differentially expressed genes in GSE64052 and GSE76068 datasets were regarded as hub genes. *CTGF* and *THBS1* were found downregulated but *RSAD2* was upregulated in ccRCC resistance to sunitinib compared with ccRCC sensitivity to sunitinib.

### Identification of miRNA-hub gene interactions associated with ccRCC resistance to sunitinib

The StarBase and TargetScan databases were applied to search common putative miRNAs targeting *CTGF*, *RSAD2*, and *THBS1*. A total of 70 common miRNAs targeting *CTGF* (Figure 2A), 10 common miRNAs targeting *RSAD2* (Figure 2B), and 176 common miRNAs targeting *THBS1* (Figure

2C). We imported *CTGF*, *RSAD2*, and *THBS1* into the survival analysis function of the StarBase database and found that only *THBS1* was correlated with the survival of ccRCC patients (n = 517,  $P = .03$ , Figure 2D). Therefore, our next analysis focused on miRNA-*THBS1* interactions associated with ccRCC resistance to sunitinib. Previous RNA-sequencing data<sup>16,23</sup> found that *miR-96-5p*, *miR-29b-3p*, and *miR-212-3p* were all upregulated in ccRCC resistance to sunitinib compared with ccRCC sensitivity to sunitinib, and three of them were putative miRNAs targeting *THBS1*. Accordingly, we imported *miR-96-5p*, *miR-29b-3p*, and *miR-212-3p* into the survival analysis function of the StarBase database (Figure 2D), and found that *miR-96-5p* (n = 517,  $P = .005$ ) and *miR-29b-3p* (n = 517,  $P < .001$ ) were correlated with the survival of ccRCC patients. Therefore, *miR-96-5p*-*THBS1* and *miR-29b-3p*-*THBS1* were investigated further.

### *THBS1* as the target gene of *miR-96-5p* and *miR-29b-3p*

The miRNA-Target co-expression function of the StarBase database showed negative Pearson correlations between *miR-96-5p*, *miR-29b-3p*, and *THBS1* in ccRCC patients (Figure 3A). Targeting *THBS1* directly by *miR-96-5p* and *miR-29b-3p* was supported by luciferase activity detection of a luciferase reporter cassette spanning the human *THBS1* 3'UTR containing either wild-type or the mutated *miR-96-5p* or *miR-29b-3p* binding site in HEK293T co-transfected with *miR-96-5p* or *miR-29b-3p* mimic. We observed that *miR-96-5p* and *miR-29b-3p* mimic transfections both reduced the luciferase activity in HEK293T transfected with pMIR-*THBS1*-wt but exerted no effect in HEK293T transfected with pMIR-*THBS1*-mut (Figure 3B).

### Expressions of *miR-96-5p*, *miR-29b-3p*, and *THBS1* in ccRCC and sunitinib resistance

For clinical validation, we sought to determine expressions of *miR-96-5p*, *miR-29b-3p*, and *THBS1* in our ccRCC cohort involving 52 pairs of tumor and non-tumor kidney tissues and their association with patient outcomes after sunitinib treatment. Results of qRT-PCR provided evidence of higher expressions of *miR-96-5p* and a lower expression of *miR-29b-3p* of *THBS1* in tumor kidney tissues than matched non-tumor kidney tissues ( $P < .05$ , Figure 4A), in tumor kidney tissues of responders than those of non-responders ( $P < .05$ , Figure 4B). More specifically, elevated expressions of *miR-96-5p*, *miR-29b-3p*, and a declined expression of *THBS1* were observed in tumor samples with advanced ccRCCs and higher Fuhrman grades ( $P < .05$ , Figure 4C, D). Pearson correlation analysis (Figure 5) yielded significantly negative correlations between *miR-96-5p* and *THBS1* ( $P < .006$ ,  $r = -0.339$ ) and between *miR-29b-3p* and *THBS1* ( $P < .05$ ,  $r = -0.421$ ).

**Figure 4.** Expressions of *miR-96-5p*, *miR-29b-3p*, and *THBS1* in ccRCC and sunitinib resistance. (A) The expressions of *miR-96-5p*, *miR-29b-3p*, and *THBS1* in tumor kidney tissues (n = 52) and matched non-tumor kidney tissues (n = 52) were determined by qRT-PCR. (B) The expressions of *miR-96-5p*, *miR-29b-3p*, and *THBS1* in tumor kidney tissues from sunitinib responders (n = 11) and non-responders (n = 8) were determined by qRT-PCR. (C) The expressions of *miR-96-5p*, *miR-29b-3p*, and *THBS1* in tumor samples with different TNM stages (n = 40 for stage I + II; n = 24 for stage III + IV) and Fuhrman grades (n = 32 for grade I + II; n = 32 for grade III + IV).

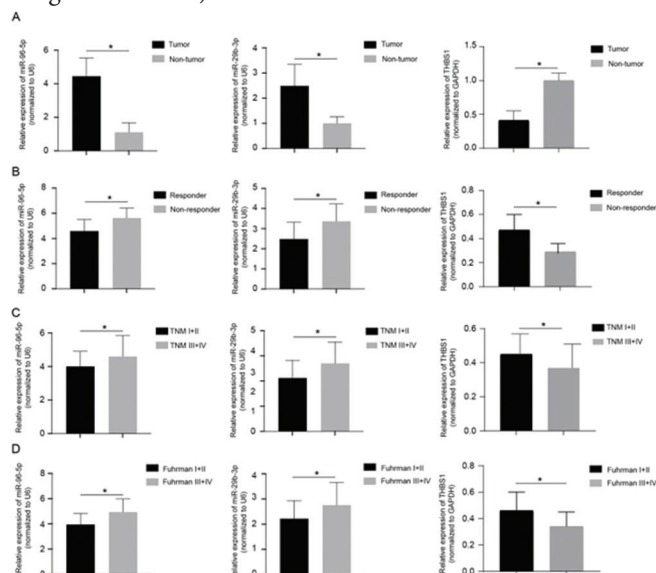
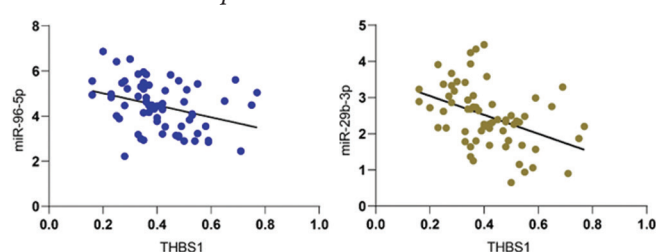


**Figure 5.** Pearson Correlation Analysis Yield Significantly Negative Correlations Between *miR-96-5p* and *THBS1* and Between *miR-29b-3p* and *THBS1*



## DISCUSSION

Due to the development of drug resistance, drug targeting therapy for ccRCC patients has a time limit for disease control. Previous evidences demonstrated that various miRNAs affected cancer progression and multi-drug resistance. In the study of colorectal cancer, down-regulated miR-145 was observed in patient-derived cancer stem cells, and miR-145 reversed SNAI1-mediated stemness and radiation resistance.<sup>24</sup> Reduced expression of miR-130a in lung cancer contributed to decline in TNF-related apoptosis-inducing ligand resistance in cancer cell lines.<sup>25</sup>

In the present study, we first confirmed differentially expressed genes between sunitinib sensitivity and sunitinib

resistance in ccRCC based on GSE64052 and GSE76068 datasets, and three hub genes including *CTGF*, *RSAD2*, and *THBS1* were involved in sunitinib resistance. Subsequently, StarBase and TargetScan databases were used to identify corresponding putative miRNAs. It was found that only *THBS1* and two miRNAs (*miR-96-5p*, *miR-29b-3p*) were relevant to the survival of ccRCC patients. Next, we determined the expression of *THBS1* in our ccRCC cohort involving tumor and matched non-tumor kidney tissues and their association with patient outcomes after sunitinib treatment. A declined expression of *THBS1* was observed in tumor samples with advanced ccRCCs and higher Fuhrman grades. *THBS1* is an endogenous angiogenesis inhibitor, which is secreted by a variety of cell types. *THBS1* overexpression reduced drug sensitivity in gastric cancer, leading to poor prognosis.<sup>27</sup> Wang et al. pointed out that in the treatment of breast cancer, up-regulation of *THBS1* after chemotherapy was associated with chemotherapy resistance in patients.<sup>28</sup> In our study, reduced *THBS1* level was found in sunitinib resistance and correlated with the survival of ccRCC patients.

In fact, a large number of studies proved the roles of miRNAs responsible for mRNA regulation in the diagnosis, prognosis, and drug resistance in RCC. Berkers et al revealed reduced expression of miR-141 provided unfavorable response to sunitinib therapy in metastatic ccRCC and the action was performed through induction of epithelial-to-mesenchymal transition.<sup>29</sup> Zhai and his team presented a study of RCC and discovered that miR-452-5p up-regulation was detrimental to prognosis, and while sunitinib reversed this negative effect.<sup>30</sup> The results in our study showed that *miR-96-5p* and *miR-29b-3p* were correlated with the survival of ccRCC patients. In previous studies, *miR-96-5p* was considered to be an oncogene which accelerated tumor progression by inhibiting the expression of tumor suppressor genes. In a study involving breast cancer, it was discovered that *miR-96-5p* suppressed tumor cell apoptosis by negatively regulating gene *FOXO3*.<sup>31</sup> A research of papillary thyroid carcinoma also confirmed the pro-oncogene function of *miR-96-5p*.<sup>32</sup> Regarding the sunitinib resistance in ccRCC, Park et al. reported an increased level of *miR-96-5p* concomitant with a decreased level of its target gene *PTEN* led to sunitinib resistance and poor prognosis in patients.<sup>23</sup> However, they only included 6 ccRCC patients consisting of 3 non-responders to sunitinib treatment and 3 responders for measuring the expression of *miR-96-5p* in ccRCC and its relationship to sunitinib resistance. Our study included tumor and matched non-tumor kidney tissues obtained from 64 ccRCC patients including 11 sunitinib responders and 8 non-responders, which strengthened the validity of *miR-96-5p* expression related to sunitinib resistance. As for *miR-29b-3p*, Pan et al. revealed that the decrease of radioresistance in tumor cells was closely related to *miR-29b-3p* overexpression, and the effect was carried out via suppressing tumor promotion genes including *RBL1*, *PIK3R1*, *AKT2*, and *Bcl-2*.<sup>33</sup>

In a previous study, Wang et al. investigated the microRNA and mRNA interaction network in cigarette smoke induced lung cancer, and found *miR-96-5p* and *THBS1* were involved in the malignant transformation progression of cancer.<sup>34</sup> *THBS1* and *miR-29b-3p* were responsible for occurrence and progression of gastric cancer.<sup>35</sup> In Dogar et al.'s study, they performed a systematic screening of predicted miRNA binding sites in the *THBS1* 3'UTR and employed chemically synthesized pre-miRNAs-a new class of pre-miRNA mimics-to show that *miR-29b* could regulate *THBS1* expression at the post-transcriptional level showing an inverse correlation in human cancer.<sup>36</sup> The present study implemented luciferase activity detection to prove the target relationship between *THBS1*, *miR-96-5p* and *miR-29b-3p*. Besides, we found higher expressions of *miR-96-5p* and *miR-29b-3p* in tumor kidney tissues than matched non-tumor kidney tissues. The findings suggest that *miR-96-5p* and *miR-29b-3p* mediate sunitinib resistance in ccRCC likely via targeting *THBS1*.

We believe that uncovering the study limitations may be helpful in interpreting our data. First, lack of a validation cohort to identify differentially expressed genes associated with ccRCC resistance to sunitinib. Secondly, functional studies *in vitro* and *in vivo* are warranted to examine the targeted inhibition on *THBS1* by *miR-96-5p* and *miR-29b-3p*. Thirdly, the depth of response analysis was exploratory and limited by the small number of patients receiving sunitinib treatment.

In conclusion, our results indicate that *THBS1* is a target gene of *miR-96-5p* and *miR-29b-3p*, which is negatively correlated with the expression levels of these two miRNAs. The *miR-96-5p*- *THBS1* and *miR-29b-3p*-*THBS1* axis are responsible for sunitinib resistance in ccRCC. However, the specific signaling pathway is still need to be determined. In the future, we will collect more ccRCC samples resistant or sensitive to ccRCC to perform RNA-sequencing or arraying for better clinical validation and functional studies.

## APPENDIX

The GSE64052 and GSE76068 datasets were downloaded from the Gene Expression Omnibus database (GEO, <http://www.ncbi.nlm.nih.gov/geo>), which is a public database. Other data used to support the findings of this study are included within the article.

## FUNDING

The project received no outside financing.

## AUTHOR DISCLOSURE STATEMENT

All authors declared no conflict of interest.

## ACKNOWLEDGEMENT

None.

## REFERENCES

- Siegel RL, Miller KD, Jemal A. Cancer statistics, 2019. *CA Cancer J Clin*. 2019;69(1):7-34. doi:10.3322/caac.21551
- Bhatt JR, Finelli A. Landmarks in the diagnosis and treatment of renal cell carcinoma. *Nat Rev Urol*. 2014;11(9):517-525. doi:10.1038/nrurol.2014.194
- Warren AY, Harrison D. WHO/ISUP classification, grading and pathological staging of renal cell carcinoma: standards and controversies. *World J Urol*. 2018;36(12):1913-1926. doi:10.1007/s00345-018-2447-8
- Makhov P, Joshi S, Ghatlani P, Kutikov A, Uzzo RG, Kolenko VM. Resistance to Systemic Therapies in Clear Cell Renal Cell Carcinoma: Mechanisms and Management Strategies. *Mol Cancer Ther*. 2018;17(7):1355-1364. doi:10.1158/1535-7163.MCT-17-1299
- Baldewijns MM, van Vlodrop IJ, Schouten LJ, Soetekouw PM, de Bruine AP, van Engeland M. Genetics and epigenetics of renal cell cancer. *Biochim Biophys Acta*. 2008;1785(2):133-155. doi:10.1016/j.bbcan.2007.12.002
- Xu WH, Xu Y, Wang J, et al. Prognostic value and immune infiltration of novel signatures in clear cell renal cell carcinoma microenvironment. *Aging (Albany NY)*. 2019;11(17):6999-7020. doi:10.18632/aging.102233
- Ricketts CJ, De Cubas AA, Fan H, et al; Cancer Genome Atlas Research Network. The Cancer Genome Atlas Comprehensive Molecular Characterization of Renal Cell Carcinoma. *Cell Rep*. 2018;23(1):313-326.e5. doi:10.1016/j.celrep.2018.03.075
- Siegel RL, Miller KD, Jemal A. Cancer Statistics, 2017. *CA Cancer J Clin*. 2017;67(1):7-30. doi:10.3322/caac.21387
- Motzer RJ, Escudier B, Tomczak P, et al. Axitinib versus sorafenib as second-line treatment for advanced renal cell carcinoma: overall survival analysis and updated results from a randomised phase 3 trial. *Lancet Oncol*. 2013;14(6):552-562. doi:10.1016/S1470-2045(13)70093-7
- Isaacsson Velho P, Nardo M, Souza MCLA, et al. Analysis of Efficacy and Toxicity Profile of First-Line Sunitinib or Pazopanib in Metastatic Clear Cell Renal Cell Carcinoma in the Brazilian Population. *J Glob Oncol*. 2018;4(4):1-10. doi:10.1200/JGO.18.00073
- Ravaud A, Motzer RJ, Pandha HS, et al; S-TRAC Investigators. Adjuvant Sunitinib in High-Risk Renal-Cell Carcinoma after Nephrectomy. *N Engl J Med*. 2016;375(23):2246-2254. doi:10.1056/NEJMoa1611406
- Molina AM, Lin X, Korytowsky B, et al. Sunitinib objective response in metastatic renal cell carcinoma: analysis of 1059 patients treated on clinical trials. *Eur J Cancer*. 2014;50(2):351-358. doi:10.1016/j.ejca.2013.08.021
- Liu Y, Cheng G, Huang Z, et al. Long noncoding RNA SNHG12 promotes tumour progression and sunitinib resistance by upregulating CDCA3 in renal cell carcinoma. *Cell Death Dis*. 2020;11(7):515. doi:10.1038/s41419-020-2713-8
- Saliminejad K, Khorram Khorshid HR, Soleymani Fard S, Ghaffari SH. An overview of microRNAs: Biology, functions, therapeutics, and analysis methods. *J Cell Physiol*. 2019;234(5):5451-5465. doi:10.1002/jcp.27486
- Elballal MS, Sallam AM, Elesawy AE, et al. miRNAs as potential game-changers in renal cell carcinoma: future clinical and medicinal uses. *Pathol Res Pract*. 2023;245:154439. doi:10.1016/j.prp.2023.154439
- Armesto M, Marquez M, Arestin M, et al. Integrated mRNA and miRNA Transcriptomic Analyses Reveals Divergent Mechanisms of Sunitinib Resistance in Clear Cell Renal Cell Carcinoma (ccRCC). *Cancers (Basel)*. 2021;13(17):4401. doi:10.3390/cancers13174401
- Li W, Li G, Cao L. Circular RNA Eps15-homology domain-containing protein 2 induce resistance of renal cell carcinoma to sunitinib via microRNA-4731-5p/ABCF2 axis. *Bioengineered*. 2022;13(4):9729-9740. doi:10.1080/21655979.2022.2059960
- Wang Z, Chang X, Zhu G, Gao X, Chang L. Depletion of lncRNA MALAT1 inhibited sunitinib resistance through regulating miR-362-3p-mediated G3BP1 in renal cell carcinoma. *Cell Cycle*. 2020;19(16):2054-2062. doi:10.1080/15384101.2020.1792667
- Moch H, Amin MB, Berney DM, et al. The 2022 World Health Organization Classification of Tumours of the Urinary System and Male Genital Organs-Part A: Renal, Penile, and Testicular Tumours. *Eur Urol*. 2022;82(5):458-468. doi:10.1016/j.eururo.2022.06.016
- Delahunt B, Sika-Paotonu D, Bethwaite PB, et al. Grading of clear cell renal cell carcinoma should be based on nucleolar prominence. *Am J Surg Pathol*. 2011;35(8):1134-1139. doi:10.1097/PAS.0b013e318220697f
- Bouchalova P, Beranek J, Lapcik P, et al. Transgelin Contributes to a Poor Response of Metastatic Renal Cell Carcinoma to Sunitinib Treatment. *Biomedicines*. 2021;9(9):1145. doi:10.3390/biomedicines9091145
- Eisenhauer EA, Therasse P, Bogaerts J, et al. New response evaluation criteria in solid tumours: revised RECIST guideline (version 1.1). *Eur J Cancer*. 2009;45(2):228-247. doi:10.1016/j.ejca.2008.10.026
- Park SE, Kim W, Hong JY, et al. miR-96-5p targets PTEN to mediate sunitinib resistance in clear cell renal cell carcinoma. *Sci Rep*. 2022;12(1):3537. doi:10.1038/s41598-022-07468-x
- Pan G, Liu Y, Shang L, Zhou F, Yang S. EMT-associated microRNAs and their roles in cancer stemness and drug resistance. *Cancer Commun (Lond)*. 2021;41(3):199-217. doi:10.1002/cac2.12138
- Acunzo M, Visone R, Romano G, et al. miR-130a targets MET and induces TRAIL-sensitivity in NSCLC by downregulating miR-221 and 222. *Oncogene*. 2012;31(5):634-642. doi:10.1038/onc.2011.260
- Isenberg JS, Roberts DD. *THBS1* (thrombospondin-1). *Atlas Genet Cytogenet Oncol Haematol*. 2020;24(8):291-299. doi:10.4267/2042/70774
- Zhang X, Huang T, Li Y, Qiu H. Upregulation of *THBS1* is Related to Immunity and Chemotherapy Resistance in Gastric Cancer. *Int J Gen Med*. 2021;14:4945-4957. doi:10.2147/IJGM.S329208
- Wang T, Srivastava S, Hartman M, et al. High expression of intratumoral stromal proteins is associated with chemotherapy resistance in breast cancer. *Oncotarget*. 2016;7(34):55155-55168. doi:10.18632/oncotarget.10894
- Berkers J, Govaere O, Wolter P, et al. A possible role for microRNA-141 down-regulation in sunitinib resistant metastatic clear cell renal cell carcinoma through induction of epithelial-to-mesenchymal transition and hypoxia resistance. *J Urol*. 2013;189(5):1930-1938. doi:10.1016/j.juro.2012.11.133
- Zhai W, Li S, Zhang J, et al. Sunitinib-suppressed miR-452-5p facilitates renal cancer cell invasion and metastasis through modulating SMAD4/SMAD7 signals. *Mol Cancer*. 2018;17(1):157. doi:10.1186/s12943-018-0906-x
- Yin Z, Wang W, Qu G, Wang L, Wang X, Pan Q. MiRNA-96-5p impacts the progression of breast cancer through targeting FOXO3. *Thorac Cancer*. 2020;11(4):956-963. doi:10.1111/1759-7714.13348
- Song HM, Luo Y, Li DF, et al. MicroRNA-96 plays an oncogenic role by targeting FOXO1 and regulating AKT/FOXO1/Bim pathway in papillary thyroid carcinoma cells. *Int J Clin Exp Pathol*. 2015;8(9):9889-9900.
- Pan D, Du Y, Li R, et al. miR-29b-3p Increases Radiosensitivity in Stemness Cancer Cells via Modulating Oncogenes Axis. *Front Cell Dev Biol*. 2021;9:741074. doi:10.3389/fcell.2021.741074
- Wang J, Yu XF, Ouyang N, et al. MicroRNA and mRNA Interaction Network Regulates the Malignant Transformation of Human Bronchial Epithelial Cells Induced by Cigarette Smoke. *Front Oncol*. 2019;9:1029. doi:10.3389/fonc.2019.01029
- Zhang S, Xiang X, Liu L, Yang H, Cen D, Tang G. Bioinformatics Analysis of Hub Genes and Potential Therapeutic Agents Associated with Gastric Cancer. *Cancer Manag Res*. 2021;13:8929-8951. doi:10.2147/CMAR.S341485
- Dogar AM, Semplicio G, Guenewig B, Hall J. Multiple microRNAs derived from chemically synthesized precursors regulate thrombospondin 1 expression. *Nucleic Acid Ther*. 2014;24(2):149-159. doi:10.1089/nat.2013.0467